

Transition formfactors $\gamma^* \rightarrow \gamma f_2(1270)$ and $\gamma^* \rightarrow \gamma a_2(1320)$ in the e^+e^- collisions

N. N. Achasov^{1,*} and A. V. Kiselev^{1,2,**}

¹Sobolev Institute for Mathematics, 630090 Novosibirsk, Russia

²Novosibirsk State University, 630090 Novosibirsk, Russia

Abstract. Transition form factors $\gamma^* \rightarrow \gamma f_2(1270)$ and $\gamma^* \rightarrow \gamma a_2(1320)$ and corresponding $e^+e^- \rightarrow \gamma^* \rightarrow f_2\gamma$ and $e^+e^- \rightarrow \gamma^* \rightarrow a_2\gamma$ cross sections are considered up to high energies. It is shown that the QCD asymptotics of the amplitudes of the $e^+e^- \rightarrow \gamma^* \rightarrow f_2\gamma$ and $e^+e^- \rightarrow \gamma^* \rightarrow a_2\gamma$ reactions can be reached only by taking into account a compensation of contributions of $\rho(770)$, $\omega(782)$ with contributions of their radial excitations. Recent BABAR measurement of the $e^+e^- \rightarrow f_2\gamma \rightarrow \pi^+\pi^-\gamma$ cross section at 10.58 GeV gives hope for detailed investigation of the $\gamma^*(s) \rightarrow f_2\gamma$ and $\gamma^*(s) \rightarrow a_2\gamma$ transition form factors at high energy region. Recent Belle data on the $\gamma^*(Q^2)\gamma \rightarrow f_2$ transition up to $Q^2 = 30 \text{ GeV}^2$ are taken into account.

It is accepted that $f_2(1270)$ and $a_2(1320)$ tensor mesons are two-quark states, $a_2 = (u\bar{u} - d\bar{d})/\sqrt{2}$ and $f_2 = (u\bar{u} + d\bar{d})/\sqrt{2}$.

The $\gamma^* \rightarrow f_2(1270)\gamma$ and $\gamma^* \rightarrow a_2(1320)\gamma$ transition form factors manifest themselves in $e^+e^- \rightarrow \gamma^* \rightarrow T\gamma$ (time-like region of γ^*) and $\gamma^*(Q^2)\gamma \rightarrow T$ (space-like region) reactions, where $T = f_2(1270)$ or $a_2(1320)$. These reactions are connected with each other, so progress in investigation of one reactions can shed light on the other reactions.

Recently BABAR presented a measurement $\sigma(e^+e^- \rightarrow f_2\gamma \rightarrow \pi^+\pi^-\gamma)$ at high-energy point [1], $\sigma(e^+e^- \rightarrow f_2\gamma \rightarrow \pi^+\pi^-\gamma, 10.58 \text{ GeV}) = 37_{-18}^{+24}$, and Belle measured the $\gamma^*(Q^2)\gamma \rightarrow f_2$ transition form factor in the space-like region for Q^2 up to 30 GeV^2 [2].

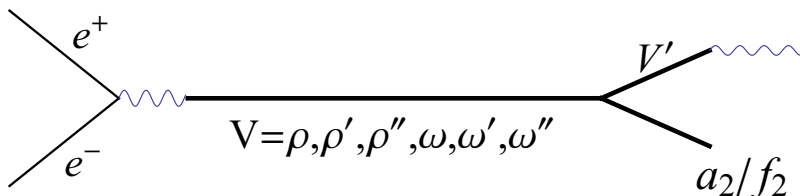


Figure 1. Diagram of $e^+e^- \rightarrow a_2(f_2)\gamma$ process.

*e-mail: achasov@math.nsc.ru

**e-mail: kiselev@math.nsc.ru

The diagram of the $e^+e^- \rightarrow \gamma^* \rightarrow T\gamma$ process is shown in Fig. 1. V and V' are appropriate vector mesons, ρ , ω and their radial excitations.

It is known that in $\gamma\gamma \rightarrow f_2 \rightarrow \pi\pi$ reaction tensor mesons are produced mainly by the photons with the opposite helicity states. This is naturally described by the Lagrangian [3]

$$L = g_{T\gamma\gamma} T_{\mu\nu} F_{\mu\sigma} F_{\nu\sigma} \quad (1)$$

where $F_{\mu\nu} = \partial_\mu A_\nu - \partial_\nu A_\mu$, $T_{\mu\nu}$ is a tensor meson T field.

In the frame of GVDM it is assumed that the effective Lagrangian of the reaction $f_2 \rightarrow VV$ is

$$L = g_{f_2 VV} T_{\mu\nu} F_{\mu\sigma}^V F_{\nu\sigma}^V \quad (2)$$

where $F_{\mu\sigma}^V = \partial_\mu V_\sigma - \partial_\sigma V_\mu$ and $V = \rho_1, \rho_2, \rho_3, \omega_1, \omega_2, \omega_3$, where $\rho_1 = \rho, \rho_2 = \rho', \rho_3 = \rho''$ and $\omega_1 = \omega, \omega_2 = \omega', \omega_3 = \omega''$.

Assuming the GVDM mechanism $e^+e^- \rightarrow \gamma^* \rightarrow (\rho + \rho' + \rho'' + \omega + \omega' + \omega'') \rightarrow f_2(\rho + \rho' + \rho'' + \omega + \omega' + \omega'') \rightarrow f_2\gamma$ one obtains [4]

$$\sigma_{e^+e^- \rightarrow f_2\gamma}(s) = \frac{4\pi^2}{9} \alpha^3 \left(1 - \frac{m_{f_2}^2}{s}\right)^3 \left(\frac{s^2}{m_{f_2}^4} + 3\frac{s}{m_{f_2}^2} + 6\right) \times \left| \frac{m_\rho^2 g_{f_2\rho\rho}}{f_\rho^2 D_\rho(s)} + \frac{m_{\rho'}^2 g_{f_2\rho'\rho'}}{f_{\rho'}^2 D_{\rho'}(s)} + \frac{m_{\rho''}^2 g_{f_2\rho''\rho''}}{f_{\rho''}^2 D_{\rho''}(s)} + \frac{m_\omega^2 g_{f_2\omega\omega}}{f_\omega^2 D_\omega(s)} + \frac{m_{\omega'}^2 g_{f_2\omega'\omega'}}{f_{\omega'}^2 D_{\omega'}(s)} + \frac{m_{\omega''}^2 g_{f_2\omega''\omega''}}{f_{\omega''}^2 D_{\omega''}(s)} \right|^2. \quad (3)$$

Here $D_V(s)$ are inverse propagators

$$D_V(s) = m_V^2 - s - i\sqrt{s}\Gamma_V(s), \quad (4)$$

the forms of widths $\Gamma_V(s)$ are described below. The constants f_V are related to e^+e^- widths as usual:

$$\Gamma(V \rightarrow e^+e^-) = \frac{4\pi\alpha^2}{3f_V^2} m_V. \quad (5)$$

In $q\bar{q}$ model $g_{f_2\rho_i\rho_i} = g_{f_2\omega_i\omega_i}$, $m_{\omega_i} = m_{\rho_i}$, $f_{\omega_i} = 3f_{\rho_i}$, this gives

$$\Gamma_{f_2 \rightarrow \gamma\gamma} = \left(\frac{10}{9}\right)^2 \frac{\pi\alpha^2}{5} \left| \frac{g_{f_2\rho\rho}}{f_\rho^2} + \frac{g_{f_2\rho'\rho'}}{f_{\rho'}^2} + \frac{g_{f_2\rho''\rho''}}{f_{\rho''}^2} \right|^2 m_{f_2}^3 = 3.03 \pm 0.35 \text{ keV} [5], \quad (6)$$

$$\sigma_{e^+e^- \rightarrow f_2\gamma}(s) = \frac{20\pi}{9} \alpha \frac{\Gamma_{f_2 \rightarrow \gamma\gamma}}{m_{f_2}^3} |F_{\gamma^* \rightarrow f_2\gamma}(s)|^2 \left(1 - \frac{m_{f_2}^2}{s}\right)^3 \left(\frac{s^2}{m_{f_2}^4} + 3\frac{s}{m_{f_2}^2} + 6\right). \quad (7)$$

Here $F_{\gamma^* \rightarrow f_2\gamma}(s)$ is a transition form factor. Since ω_i contributions are suppressed, we neglect the difference between Γ_{ω_i} and Γ_{ρ_i} in $D_{\omega_i}(s)$ to simplify the formula.

Let's denote $a_{f_2} = g_{f_2\rho'\rho'} f_{\rho'}^2 / g_{f_2\rho\rho} f_\rho^2$ and $b_{f_2} = g_{f_2\rho''\rho''} f_{\rho''}^2 / g_{f_2\rho\rho} f_\rho^2$. One has

$$F_{\gamma^* \rightarrow f_2\gamma}(s) = \frac{1}{1 + a_{f_2} + b_{f_2}} \left(\frac{m_\rho^2}{D_\rho(s)} + a_{f_2} \frac{m_{\rho'}^2}{D_{\rho'}(s)} + b_{f_2} \frac{m_{\rho''}^2}{D_{\rho''}(s)} \right). \quad (8)$$

The QCD asymptotics of $\sigma(e^+e^- \rightarrow \text{light hadrons})$ at $s \rightarrow \infty$ is equal to $\sum_f Q_f^2 4\pi\alpha^2/s$ to within logarithms (Q_f are charges of u, d , and s quarks). Due to asymptotic freedom at $s \rightarrow \infty$ imaginary part of $D_V(s)$ vanishes

$$\text{Im}(D_V(s)) = -\sqrt{s}\Gamma_V(s) \rightarrow 0; \quad \frac{1}{D_V(s)} \rightarrow \frac{1}{m_V^2 - s}. \quad (9)$$

It means that $F_{\gamma^* \rightarrow f_2 \gamma}(s) \sim 1/s^2$, i.e.

$$m_p^2 + a_{f_2} m_{\rho'}^2 + b_{f_2} m_{\rho''}^2 = 0 \quad (10)$$

to suppress asymptotics $\sim 1/s$ in Eq. 8.

Note the analogous condition was obtained in Refs. [6, 7] after taking into account the QCD based asymptotics of the $\gamma^*(Q^2)\gamma \rightarrow a_2$ amplitude.

The Belle Collaboration presented 3 data sets for each helicity difference $\lambda \equiv |\lambda_{\gamma^*} - \lambda_\gamma| = 0, 1, 2$. These data were described in Ref. [7] with $b_{f_2} = 0$. To take ρ'' into account it is enough to modify $\gamma^*(Q^2)\gamma \rightarrow f_2$ transition form factor (Eq. (10) of that paper):

$$F_T(Q) \rightarrow F_T(Q) = \frac{1}{1 + a_{f_2} + b_{f_2}} \left(\frac{1}{1 + \frac{Q^2}{m_p^2}} + \frac{a_{f_2}}{1 + \frac{Q^2}{m_{\rho'}^2}} + \frac{b_{f_2}}{1 + \frac{Q^2}{m_{\rho''}^2}} \right). \quad (11)$$

This gives two minimums of the χ^2 function, constructed for the Belle data: $b_{f_2} = 0.082 \pm 0.025$ and $b_{f_2} = 0.740 \pm 0.011$, see Fig. 2.

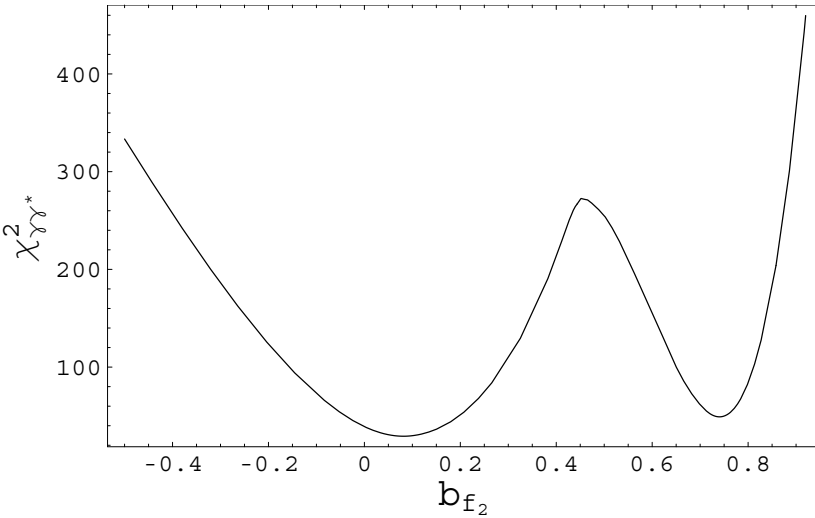


Figure 2. χ^2 function for Belle data on $\gamma^* \gamma \rightarrow f_2$ transition form factor.

Let's consider three cases:

- 1) $(a_{f_2}, b_{f_2}) = (-0.393, 0.082)$ - best minimum of the χ^2 function ($\chi^2/n.d.f. = 29.3/28$);
- 2) $(a_{f_2}, b_{f_2}) = (-1.3, 0.74)$ - second minimum of the χ^2 function ($\chi^2/n.d.f. = 49.1/28$);
- 3): $(a_{f_2}, b_{f_2}) = (-0.28, 0)$ - no ρ'' contribution ($\chi^2/n.d.f. = 39.1/29$).

Recently the $e^+e^- \rightarrow f_2 \gamma \rightarrow \pi^+ \pi^- \gamma$ cross section was measured at BABAR at 10.58 GeV: $\sigma(\pi^+ \pi^- \gamma)_{10.58} \equiv \sigma(e^+ e^- \rightarrow f_2 \gamma \rightarrow \pi^+ \pi^- \gamma, 10.58 \text{ GeV}) = 37_{-18}^{+24} \text{ fb}$.

Taking into account $Br(f_2 \rightarrow \pi^+ \pi^-) \approx 56.5\%$ and $D_V(s) \rightarrow m_V^2 - s$ at $s \rightarrow \infty$, we find $\sigma(\pi^+ \pi^- \gamma)_{10.58} = 1.0 \text{ fb}$ for $b_{f_2} = 0.082$, $\sigma(\pi^+ \pi^- \gamma)_{10.58} = 3.8 \text{ fb}$ for $b_{f_2} = 0.74$ and $\sigma(\pi^+ \pi^- \gamma)_{10.58} = 1.5$

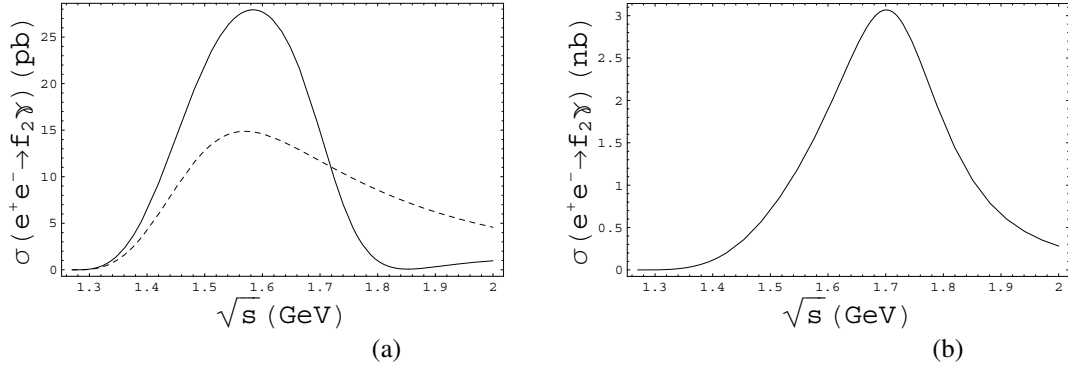


Figure 3. The $e^+e^- \rightarrow f_2\gamma$ cross section up to 2 GeV. (a) Solid line is for $(a_{f_2}, b_{f_2}) = (-0.393, 0.082)$, dashed line is for $(a_{f_2}, b_{f_2}) = (-0.28, 0)$ (ρ'' is absent). (b) The plot for $(a_{f_2}, b_{f_2}) = (-1.3, 0.74)$.

fb for $b_{f_2} = 0$. The elaboration of the pioneer measurement of $\sigma(\pi^+\pi^-\gamma)_{10.58}$ is important for the $\gamma^* \rightarrow \gamma f_2/a_2$ transition form factor investigations.

The $e^+e^- \rightarrow f_2\gamma$ cross section Eq. (7) for all three cases under consideration is shown in Figs. 3 and 4. In vector propagators Eq. (4) we use constant widths taken from Ref. [5] below 2 GeV and zero widths above 5 GeV. Dashed lines show continuation of these curves to the intermediate region.

The treatment of the $e^+e^- \rightarrow \gamma^* \rightarrow a_2\gamma$ cross section is similar:

$$\begin{aligned} \sigma_{e^+e^- \rightarrow a_2\gamma}(s) = & \frac{\pi^2}{9} \alpha^3 \left(1 - \frac{m_{a_2}^2}{s}\right)^3 \left(\frac{s^2}{m_{a_2}^4} + 3\frac{s}{m_{a_2}^2} + 6\right) \times \\ & \left| \frac{m_{\rho}^2 g_{a_2\rho\omega}}{f_{\rho} f_{\omega} D_{\rho}(s)} + \frac{m_{\omega}^2 g_{a_2\rho\omega}}{f_{\rho} f_{\omega} D_{\omega}(s)} + \frac{m_{\rho'}^2 g_{a_2\rho'\omega'}}{f_{\rho'} f_{\omega'} D_{\rho'}(s)} + \frac{m_{\omega'}^2 g_{a_2\rho'\omega'}}{f_{\rho'} f_{\omega'} D_{\omega'}(s)} + \right. \\ & \left. \frac{m_{\rho''}^2 g_{a_2\rho''\omega''}}{f_{\rho''} f_{\omega''} D_{\rho''}(s)} + \frac{m_{\omega''}^2 g_{a_2\rho''\omega''}}{f_{\rho''} f_{\omega''} D_{\omega''}(s)} \right|^2, \end{aligned} \quad (12)$$

$$\Gamma_{a_2 \rightarrow \gamma\gamma} = \frac{4\pi\alpha^2}{5} \left| \frac{g_{a_2\rho\omega}}{f_{\rho} f_{\omega}} + \frac{g_{a_2\rho'\omega'}}{f_{\rho'} f_{\omega'}} + \frac{g_{a_2\rho''\omega''}}{f_{\rho''} f_{\omega''}} \right|^2 m_{a_2}^3 = 1.00 \pm 0.06 \text{ keV [5]}. \quad (13)$$

Denoting $a_{a_2} = g_{a_2\rho'\omega'} f_{\rho} f_{\omega} / g_{a_2\rho\omega} f_{\rho'} f_{\omega'}$ and $b_{a_2} = g_{a_2\rho''\omega''} f_{\rho} f_{\omega} / g_{a_2\rho\omega} f_{\rho''} f_{\omega''}$ one gets

$$\sigma_{e^+e^- \rightarrow a_2\gamma}(s) = \frac{20\pi}{9} \alpha \frac{\Gamma_{a_2 \rightarrow \gamma\gamma}}{m_{a_2}^3} \left| F_{\gamma^* \rightarrow a_2\gamma}(s) \right|^2 \left(1 - \frac{m_{a_2}^2}{s}\right)^3 \left(\frac{s^2}{m_{a_2}^4} + 3\frac{s}{m_{a_2}^2} + 6\right) \quad (14)$$

with transition form factor

$$\begin{aligned} F_{\gamma^* \rightarrow a_2\gamma}(s) = & \frac{1}{2(1 + a_{a_2} + b_{a_2})} \times \\ & \left(\frac{m_{\rho}^2}{D_{\rho}(s)} + \frac{m_{\omega}^2}{D_{\omega}(s)} + a_{a_2} \frac{m_{\rho'}^2}{D_{\rho'}(s)} + a_{a_2} \frac{m_{\omega'}^2}{D_{\omega'}(s)} + b_{a_2} \frac{m_{\rho''}^2}{D_{\rho''}(s)} + b_{a_2} \frac{m_{\omega''}^2}{D_{\omega''}(s)} \right) \end{aligned} \quad (15)$$

and the asymptotic condition $m_{\rho}^2 + a_{a_2} m_{\rho'}^2 + b_{a_2} m_{\rho''}^2 = 0$.

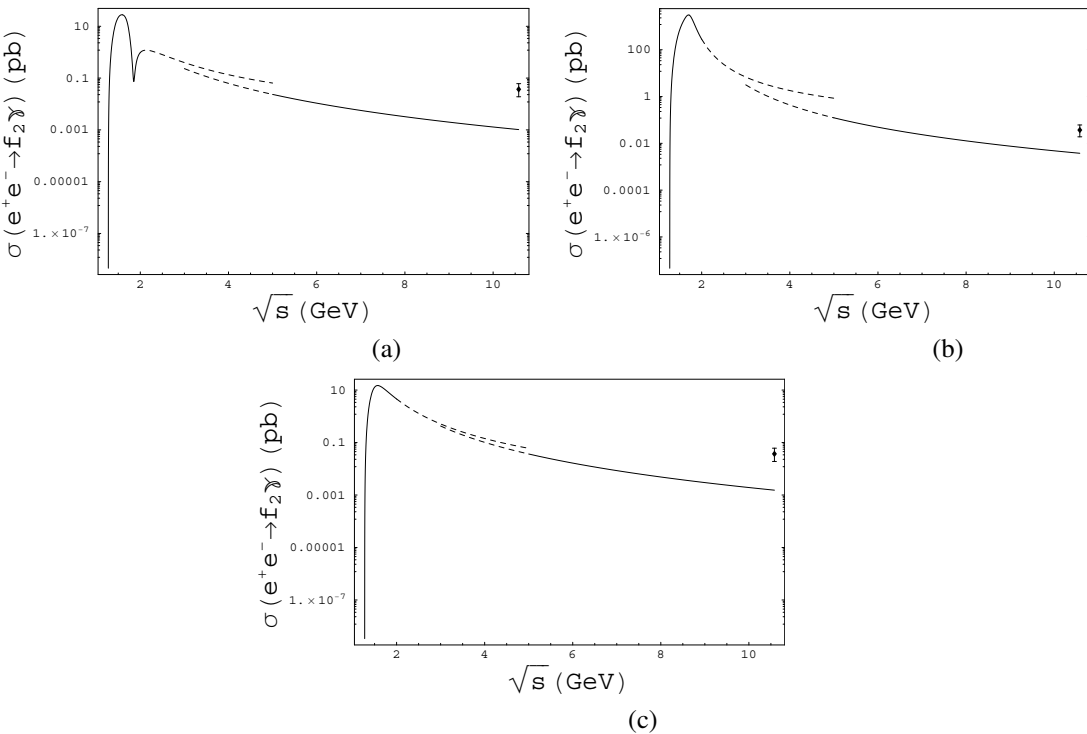


Figure 4. The $e^+e^- \rightarrow f_2\gamma$ cross section up to 10.58 GeV. In each logarithmic plot solid line below 2 GeV is drawn with constant vector widths taken from Ref. [5], solid line above 5 GeV is drawn with zero vector widths, dashed lines are their continuations. The experimental BaBar point [1] is shown also. (a) $(a_{f_2}, b_{f_2}) = (-0.393, 0.082)$, (b) $(a_{f_2}, b_{f_2}) = (-1.3, 0.74)$, (c) $(a_{f_2}, b_{f_2}) = (-0.28, 0)$ (ρ'' is absent).

In the naive $q\bar{q}$ model for $i = 1, 2, 3$ $g_{a_2\rho_i\omega_i} = g_{f_2\rho_i\rho_i}$. It means that in our approach $a_{a_2} = a_{f_2}$, $b_{a_2} = b_{f_2}$.

The resulting cross-section for the same sets of (a_{a_2}, b_{a_2}) as for $e^+e^- \rightarrow f_2(1270)\gamma$ reaction is shown in Fig. 5.

It is natural that our $q\bar{q}$ consideration agrees with QCD requirement for high s

$$\frac{\sigma(e^+e^- \rightarrow f_2\gamma, s)}{\sigma(e^+e^- \rightarrow a_2\gamma, s)} = \frac{25}{9} \quad (16)$$

and the well-known relation being in perfect agreement with the data

$$\frac{\Gamma(f_2 \rightarrow \gamma\gamma)}{\Gamma(a_2 \rightarrow \gamma\gamma)} = \frac{25}{9} \frac{m_{f_2}^3}{m_{a_2}^3} \approx \frac{25}{9}. \quad (17)$$

The above-mentioned BABAR measurement $\sigma(e^+e^- \rightarrow f_2\gamma \rightarrow \pi^+\pi^-\gamma, 10.58 \text{ GeV}) = 37_{-18}^{+24} \text{ fb}$ gives

$$\sigma(e^+e^- \rightarrow a_2\gamma, 10.58 \text{ GeV}) = 24_{-11}^{+15} \text{ fb}. \quad (18)$$

Brief summary and conclusions:

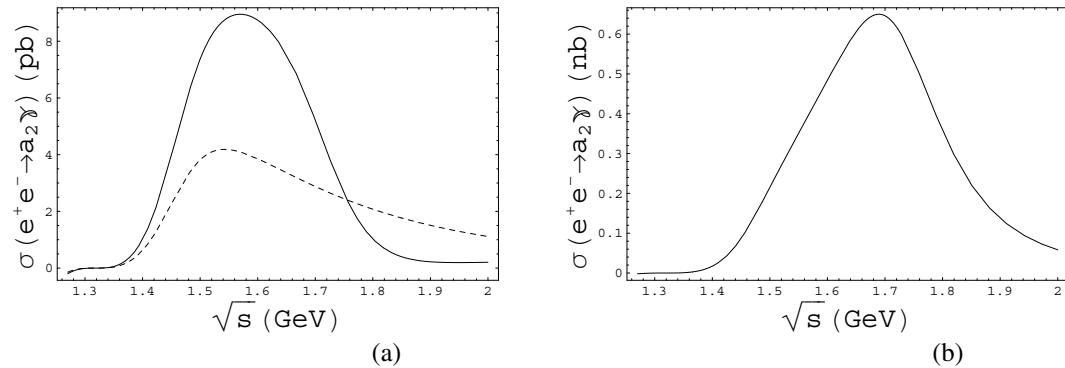


Figure 5. The $e^+e^- \rightarrow a_2\gamma$ cross section. (a) Solid line is for $(a_{a_2}, b_{a_2}) = (-0.393, 0.082)$, dashed line is for $(a_{a_2}, b_{a_2}) = (-0.28, 0)$. (b) The plot for $(a_{a_2}, b_{a_2}) = (-1.3, 0.74)$.

1. It is shown that the QCD asymptotics of the amplitudes of the reactions $e^+e^- \rightarrow \gamma^* \rightarrow f_2\gamma$ and $e^+e^- \rightarrow \gamma^* \rightarrow a_2\gamma$ can be reached only by taking into account a compensation of contributions of $\rho(770)$, $\omega(782)$ with contributions of their radial excitations.
2. The ρ and ω excitation contribution to the $e^+e^- \rightarrow f_2\gamma$ and $e^+e^- \rightarrow a_2\gamma$ cross sections is essential and allows the experimental investigation of $e^+e^- \rightarrow \eta\pi^0\gamma$ and $e^+e^- \rightarrow \pi^0\pi^0\gamma$ processes, for example, at VEPP-2000 collider. Note that the best channel to study the a_2 production is the $e^+e^- \rightarrow a_2\gamma \rightarrow \rho\pi\gamma$ because $Br(a_2 \rightarrow \rho\pi) = 70\%$ and the background is expected to be small.
3. At the BABAR energy (10.58 GeV) our estimation of the $e^+e^- \rightarrow f_2\gamma \rightarrow \pi^+\pi^-\gamma$ cross section, based on the Belle data about the $\gamma^*(Q^2)\gamma \rightarrow f_2 \rightarrow \pi^+\pi^-$ cross section, is much less than the average BABAR value, but the experimental error is half of the average value, so no conclusions concerning this disagreement could be done now. Anyway, the pioneer BABAR measurement gives hope that the detailed investigation of the $\gamma^*(s) \rightarrow f_2\gamma$ and $\gamma^*(s) \rightarrow a_2\gamma$ transition form factors at high energy region is possible.

This work was supported in part by RFBR, Grant No. 16-02-00065, and the Presidium of RAS project No. 0314-2015-0011.

References

- [1] J. P. Lees et al (BABAR Collaboration), Phys. Rev. D92 (2015) 072015.
- [2] M. Masuda *et al.* (Belle Collaboration), Phys. Rev. D93 (2016) 032003.
- [3] N.N. Achasov and V.A. Karnakov, Z. Phys. C30 (1986) 141.
- [4] N.N. Achasov, A.I. Goncharenko, A.V. Kiselev, and E.V. Rogozina, Phys. Rev. D88, (2013) 114001; Erratum-ibid. D89 (2014) 059906.
- [5] K.A. Olive *et al.* (Particle Data Group), Chin. Phys. C38 (2014) 090001.
- [6] N.N. Achasov, A.V. Kiselev, and G.N. Shestakov, Phys. At. Nucl. 79 (2016), 397.
- [7] N.N. Achasov, A.V. Kiselev and G.N. Shestakov, Pis'ma Zh. Eksp. Teor. Fiz. 102 (2015) 655 [JETP Lett. **102** (2015) 571], arXiv:1509.09150.